THE STRUCTURE AND EVOLUTION OF CORONAL HOLES

A. F. TIMOTHY* and A. S. KRIEGER
American Science and Engineering, Inc., Cambridge, Mass., U.S.A.
and
G. S. VAIANA
*Center for Astrophysics**, Cambridge, Mass., U.S.A.*

(Received 30 October, 1974; in revised form 14 January, 1975)

Abstract. When observed at soft X-ray wavelengths coronal holes are seen as open features, devoid of X-ray emission and bounded by apparently divergent coronal loop structures. Inspection of the topology of the photospheric magnetic fields associated with these features suggests that holes are formed when the remnants of active region fields, emerging in both hemispheres over a period of several solar rotations, combine to form a large area of essentially unipolar field. Remnants of opposite polarity fields surround these features resulting in a divergent magnetic configuration at the hole boundaries. Holes are seen to form and evolve while the large scale divergent field pattern is reinforced and to close when large scale remnants occur which disrupt the general field pattern. Two types of holes are observed in the early Skylab observations. The first are elongated features which are aligned approximately north-south extending from one solar pole to a polar filament channel in the opposite hemisphere. The polar holes and somewhat lower latitude holes appear to lie in unipolar areas which are completely confined by opposite polarity fields.

Studies of the rotation properties of an elongated hole, which extended from the north pole to a latitude of approximately 20°S, showed it to rotate with a synodic rate of $(13.25 \pm 0.03) - (0.4 \pm 0.1 \sin^2 \phi$ deg day^{-1}. Possible explanations for the almost rigid rotational characteristics of this feature are discussed.

1. Introduction

Soft X-ray observations of the quiet corona reveal the presence of features which are devoid of emission and are bounded by apparently diverging large scale loop structures giving them a characteristically open appearance (Vaiana *et al.*, 1973a). These open features, which are also seen as areas of reduced electron density in K-coronameter data (Altschuler *et al.*, 1972) and metric radio scans (Dulk and Sheridan, 1974) and reduced emission in certain extreme ultraviolet (EUV) lines, (Munro and Withbroe, 1972; Neupert and Pizzo, 1974) and in the D_3(5876 Å) line and 10830 Å line of He I (Harvey *et al.*, 1974) have been given the name 'coronal holes'.

High resolution observations of the coronal structures associated with these holes were first obtained by the AS&E group in sounding rocket flights on March 7 and November 24, 1970 (Krieger *et al.*, 1973). In the former case a hole located near the south west limb could be traced into the outer corona in comparisons made between the soft X-ray images and white light eclipse observations (Van Speybroeck *et al.*, 1970). Analysis of the physical characteristics of the hole seen on November 24 showed it to have a reduced emission scale height which was about half that of other coronal

* Present address: NASA Headquarters, Washington, D.C.
** Harvard College Observatory – Smithsonian Astrophysical Observatory.

Solar Physics **42** (1975) 135–156.

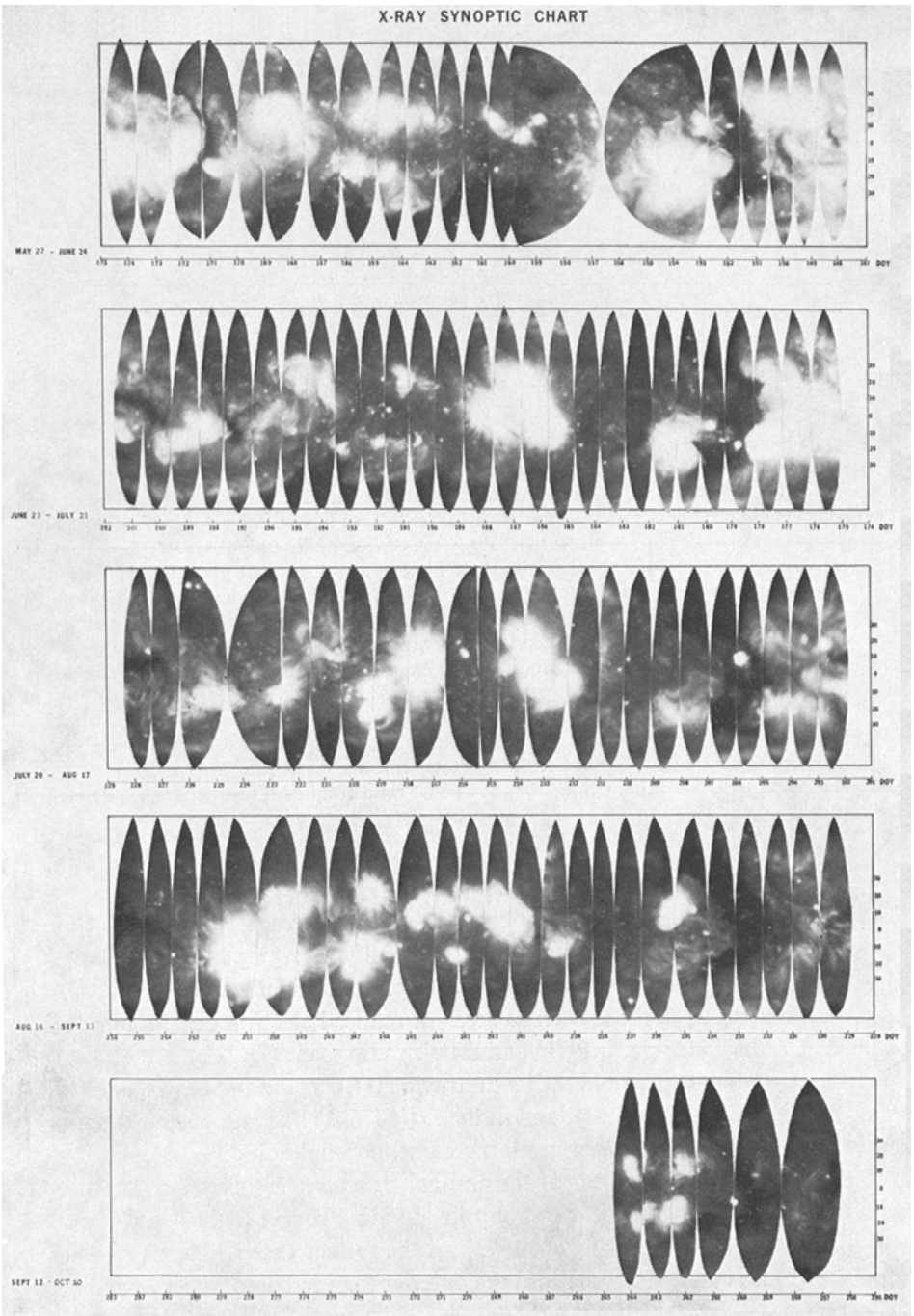

Fig. 1. A synoptic presentation of data obtained by the AS&E X-ray spectrographic telescope experiment during the first two Skylab missions. The chart is formed from segments taken from the central portion of X-ray photographs obtained at approximately 24 h intervals. The width of the segments is proportional to the time interval between selected frames and is typically 13.3° in longitude. Wider swaths correspond to periods in which data gaps occur.

structures. The interpretation of this scale height assumed that the hole plasma was in hydrostatic equilibrium along open field lines perpendicular to the surface. Under these conditions the barometric equation yielded a 'temperature' of 1.3×10^6K for the hole showing it to be cool compared with the large scale closed coronal structures surrounding it. The hole was also identified as the possible source of a recurrent high velocity stream in the solar wind.

Results obtained by the AS&E X-ray telescope experiment on the Apollo Telescope Mount (Vaiana *et al.*, 1973b) have enabled temporal variations in the structure of the large scale corona to be studied for the first time. The form and long term development of the quiet corona for a period from May 28 to September 21, 1973 are displayed by means of a 'synoptic chart' which is shown in Figure 1. This chart is formed from the central disk segments of daily images of the solar corona taken through our broadest bandpass filter (3–32 Å; 44–54 Å). The width of each segment is approximately 13.3° and is proportional to the time interval between successive 'synoptic' exposures. The rows of the chart are spaced at 27 day intervals to enable the changes in structure of selected solar features to be compared on successive rotations.

Two holes were present at the north and south solar poles during the five rotation periods for which data have been analyzed to date. In addition, two holes are seen to extend southward from the north polar hole to latitudes of approximately 20°S. Of these, one is very similar in character to the hole observed on November 24, 1970. The second is a narrow feature which was seen at central meridian passage (CMP) on day 171. This feature is apparently the remnant of a large hole which was visible for many previous rotations in the Fe XV (284 Å) extreme ultraviolet spectroheliograms which are obtained with the GSFC experiment on OSO-7 (*Solar Geophysical Data*, 1973). The EUV observations of this feature are shown, together with corresponding X-ray images, in Figures 2a and 2b. An additional small hole is seen to form at near equatorial latitudes by day 201 and to expand in size during the subsequent period for which data are available.

In this preliminary discussion of the structure and evolution of coronal holes we investigate typical coronal configurations which result in the formation of these features. We also follow the evolution of one particular hole as a function of time and investigate its rotational properties at latitudes ranging from 20°S to 50°N. Finally, we explore possible mechanisms which may account for the almost rigid rotational characteristics displayed by this feature.

2. Results

2.1. Structure

The first coronal hole observed during the Skylab mission is shown in Figure 3a. For ease of reference it is given the title CH1. The absence of large scale emitting features within the hole and its apparently 'open' nature are immediately apparent. The hole, which is centered at Carrington longitude 15°, extends from the north pole to approximately 20°S and is of the order of 15° wide at the equator. It is bounded in the

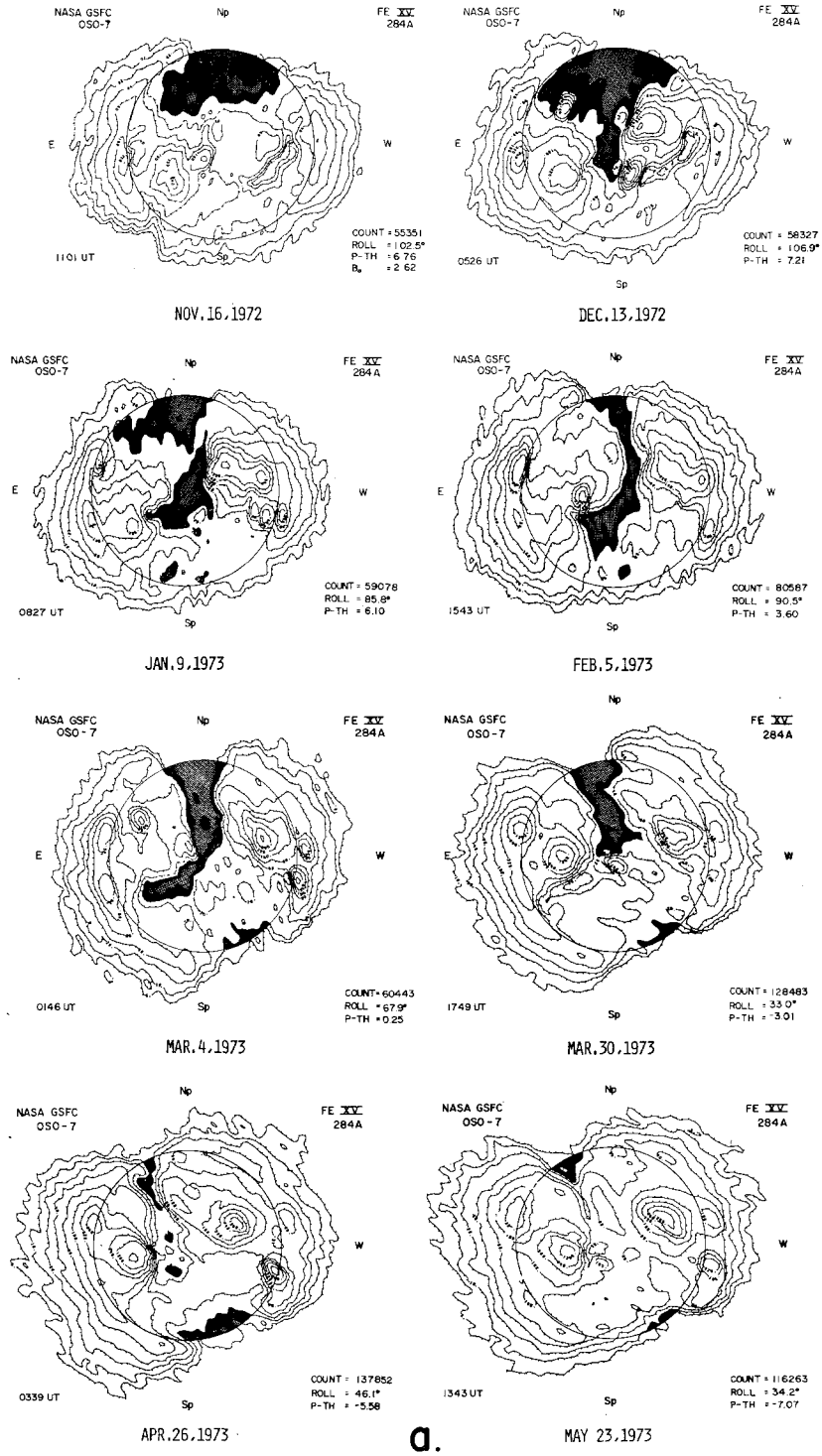

a.

Fig. 2. (a) The evolution of an elongated coronal hole, traced back through eight solar rotations using Fe xv (284 Å) extreme ultraviolet spectroheliograms obtained with the GSFC experiment on OSO-7 and published in *Solar Geophysical Data*. Areas of the disk with intensities lying below the two lowest contour levels (10 and 5 counts) are shaded black and grey respectively to indicate the

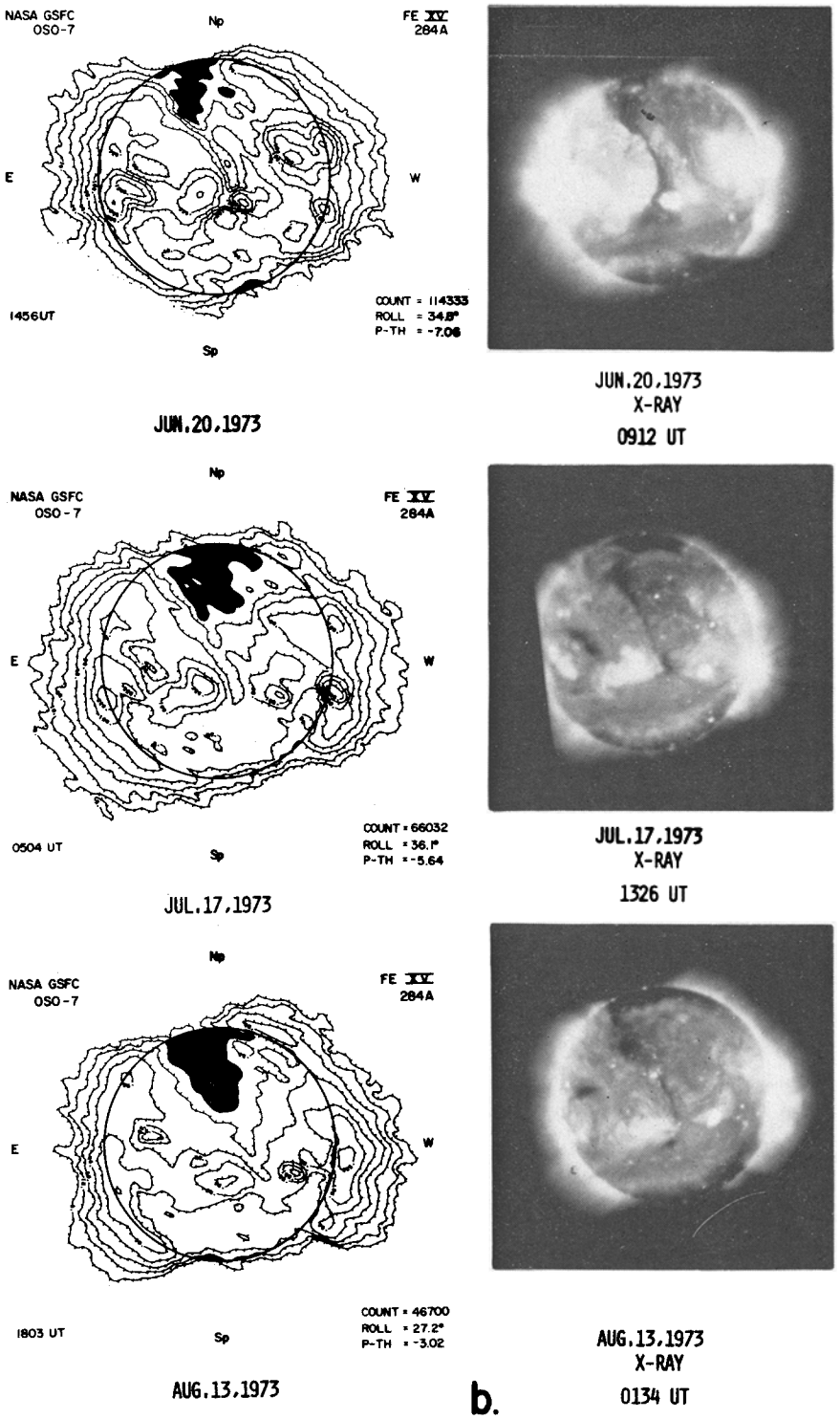

position of the hole. (b) A comparison of Fe xv (284 Å) extreme ultraviolet spectroheliograms and near simultaneous soft X-ray observations of the solar coronal taken in the 3–32 Å and 44–54 Å range. The data cover three successive solar rotations and illustrate the relationship between the low intensity contours in the Fe xv images and coronal holes observed at soft X-ray wavelengths.

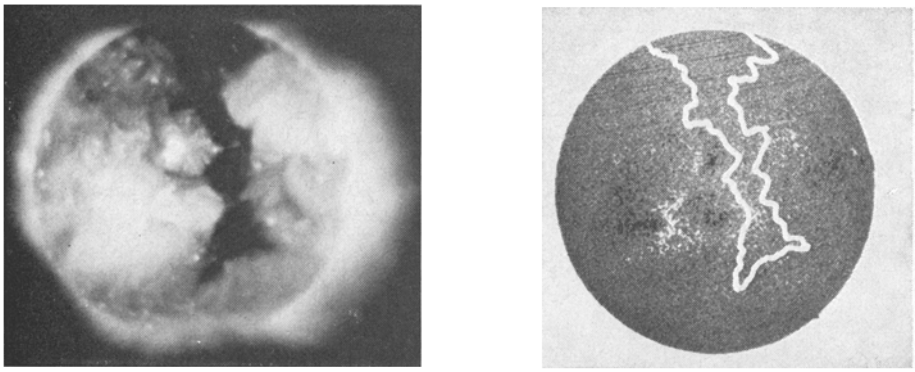

a. b.

Fig. 3. (a) An image of the solar corona, covering the wavelength range 3–32 Å and 44–54 Å obtained on 1 June 1973 at 1424 UT. (b) The Kitt Peak magnetogram for 1 June 1973, 1445 UT (courtesy of Dr J. Harvey and Dr W. Livingston of Kitt Peak National Observatory). An outline of the X-ray coronal hole is super-imposed on the magnetic field.

south, west and northeast by arcades of closed loop structures usually characteristic of filament channels (Vaiana *et al.*, 1973a). Active regions form its main eastern boundaries. The tendency for the coronal loop structures surrounding the hole to arch away from it, both in the active regions and in the filament channels, again suggests an associated divergent field configuration similar to that computed by Newkirk *et al.* (1973) for the November 24, 1970 feature.

Inspection of the photospheric magnetic field configuration associated with the hole (Figure 3b) shows it to have a dominant field of positive (white) polarity. This is the 'following' polarity for northern hemisphere active regions in this solar cycle. The polarity of the north polar hole is also assumed to be predominantly positive since it merges with CH1 while the south polar hole polarity is assumed to be negative since this hole is separated from CH1 by a filament channel. This latter fact may be confirmed by inspection of the southern hemisphere magnetic fields observed during the period June 9–11, 1973 (days 160–162) when the south polar hole extended northward to near equatorial latitudes. The band of positive field in which CH1 is located is surrounded by features with predominantly negative photospheric longitudinal field polarity. In the corona, this leads to the divergent field configuration deduced from the geometry of the boundary structures. It should be noted that the positions of the coronal structures which demarcate the boundaries of the hole are by no means evident in the magnetogram and that well defined network patterns, with field strengths in excess of 50 gauss, are present in the hole region of the magnetogram.

Small, brightly emitting features, called X-ray bright points, can be seen distributed over the entire disk and are particularly visible within the hole itself. It has been shown (Golub *et al.*, 1974) that bright points are distributed uniformly as a function of both

latitude and longitude and are not formed preferentially in holes. Furthermore, these features, which are associated with small areas of bipolar field, have a mean lifetime of 8 hours compared with a lifetime of several solar rotations for large scale features. This fact, and the obviously small scale of the magnetic fields involved imply that the presence of bright points has little effect on the general large scale field patterns or on the coronal structures associated with them.

2.2. Formation

Since both the elongated holes seen during the first two Skylab missions were present on the solar disk at the commencement of the first manned mission there are no ATM observations of the birth of these features. It is, however, possible to infer the history of formation of CH1 from data obtained from other sources. A comparison of the AS&E X-ray observations with Fe XV (284 Å) spectroheliograms obtained by the NASA Goddard Space Flight Center experiment on OSO-7 (*Solar Geophysical Data*, April–June, 1973) is shown in Figure 4. It may be seen that the position of the hole can be inferred from the two lowest contour levels in the EUV maps. Using this fact and tracing the feature back over several previous solar rotations, we conjecture that the hole formed only one rotation prior to our first observations.

Mt. Wilson magnetograms taken on the two previous central meridian passages of the longitude of the hole are shown in Figures 5b and 5c. The schematic diagram in Figure 5a illustrates the active region geometry which might have produced and reinforced the large scale magnetic field pattern with which CH1 is associated. Active regions emerge on either side of the equator, the regions in the north slightly preceding those in the south. Subsequent diffusion of the active region fields (Babcock, 1961; Leighton, 1964) results in the formation of the unipolar swath. As predicted, the 'following' polarity in either hemisphere tends poleward while the 'preceding' polarity tends more toward the equator. The result is a band of positive polarity from the north pole to 20°S. A long lived filament channel, whose northern edge may clearly be seen as a band of black (positive) field aligned approximately east-west in the southern hemisphere in Figure 5c forms the southern boundary of the feature. Once the unipolar swath has been established at photospheric levels, the resulting divergent coronal field pattern presumably leads to the formation of the coronal hole.

It is apparent from the schematic diagram in Figure 5 that a displacement of the northern and southern active regions such that the southern region precedes the northern region should also result in a large scale pattern conducive to hole formation. In this case however, the hole should be of opposite polarity and should extend to the opposite pole (assuming the condition to occur during the same phase of the solar cycle). The November 24, 1970 hole provides a test of this hypothesis. A schematic diagram of the proposed active region geometry is shown in Figure 6 together with Mt. Wilson magnetograms for four solar rotations from September 3 to November 23, 1970. The soft X-ray image obtained from a sounding rocket on November 24, 1970 is also shown. It may be seen that in this case a band of negative (dotted) field remnants is formed stretching from north of the equator towards the south pole and

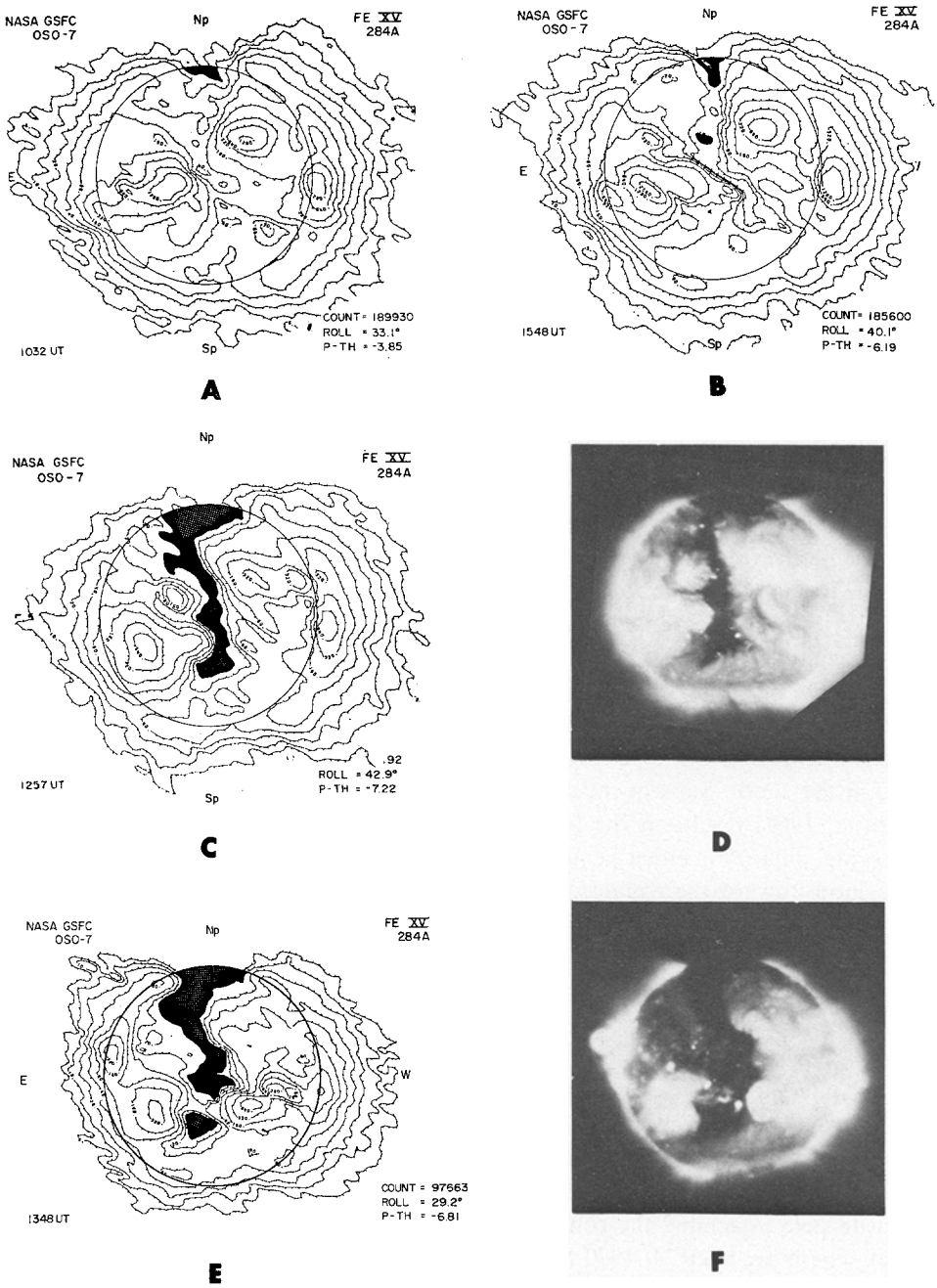

Fig. 4. (a, b) Fe xv (284 Å) extreme ultraviolet spectroheliograms of approximately Carrington longitude 15° showing the form of the hole, CH1, for two rotations prior to the commencement of the first Skylab mission. (c, d, e, f) A comparison of extreme ultraviolet and soft X-ray (3–32 and 44–54 Å) observations of the feature during the first two rotations observed from Skylab (the extreme ultraviolet maps are obtained by the GSFC experiment on OSO-7 and are published in *Solar Geophysical Data*, 1973).

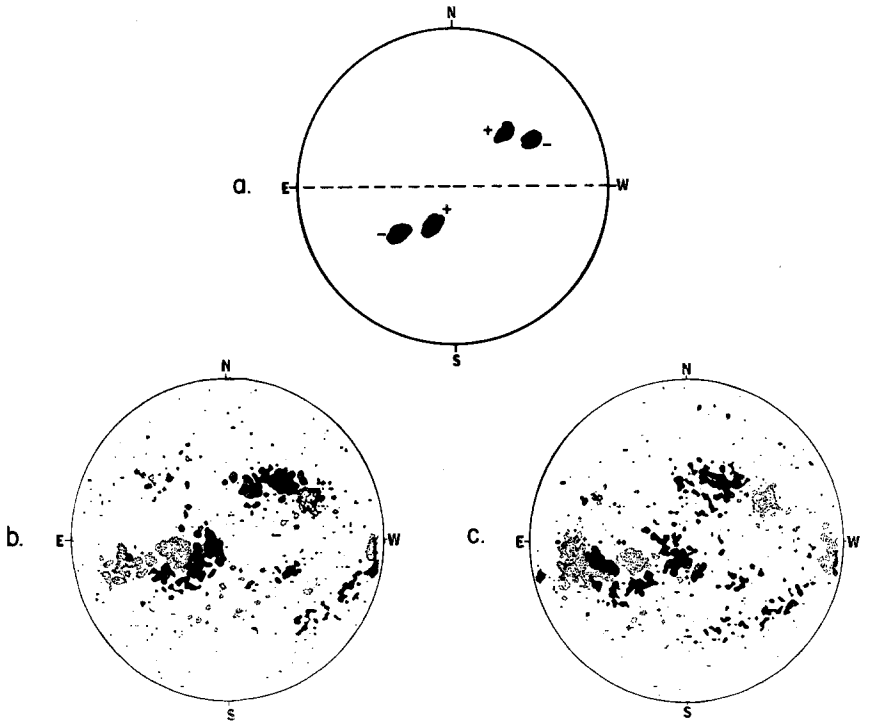

Fig. 5. (a) A schematic diagram of the active region field geometry resulting in the formation of the large scale pattern associated with CH1. (b, c) Mt. Wilson magnetograms for April 7, 1973 and May 4, 1973, respectively. Magnetic field convention: solid=plus polarity; dotted=minus polarity (Mt. Wilson magnetograms are taken from *Solar Geophysical Data*, 1973).

that the successive emergence of active regions generally reinforces the pattern. The emergence of small active regions within the unipolar band, which is seen to occur on October 28, 1970, appears to have had little effect on the large scale pattern although some diffuse remnants of the regions appear visible within the soft X-ray hole. Discrete bands of positive (black) field border the feature. The hole is terminated in the north by a filament channel, which is only clearly visible in the X-ray image, and it appears to extend southward implying that the dominant polarity of the south pole was negative at that time.

Although the formation of an 'elongated' (north-south aligned) hole was not observed during the first and second Skylab missions, a smaller 'confined' hole was seen to develop at near equatorial latitudes during this time. Figure 7 shows the central meridian passage of this feature on five successive solar rotations from May 28, 1973 to September 13, 1973. The Mt. Wilson magnetograms corresponding to this hole (termed CH2 in this paper) are shown in Figure 8. It may be seen that in this case the area of unipolar (negative) magnetic field in which CH2 is formed lies within approximately 20° of the equator and is bounded on all sides by large scale positive

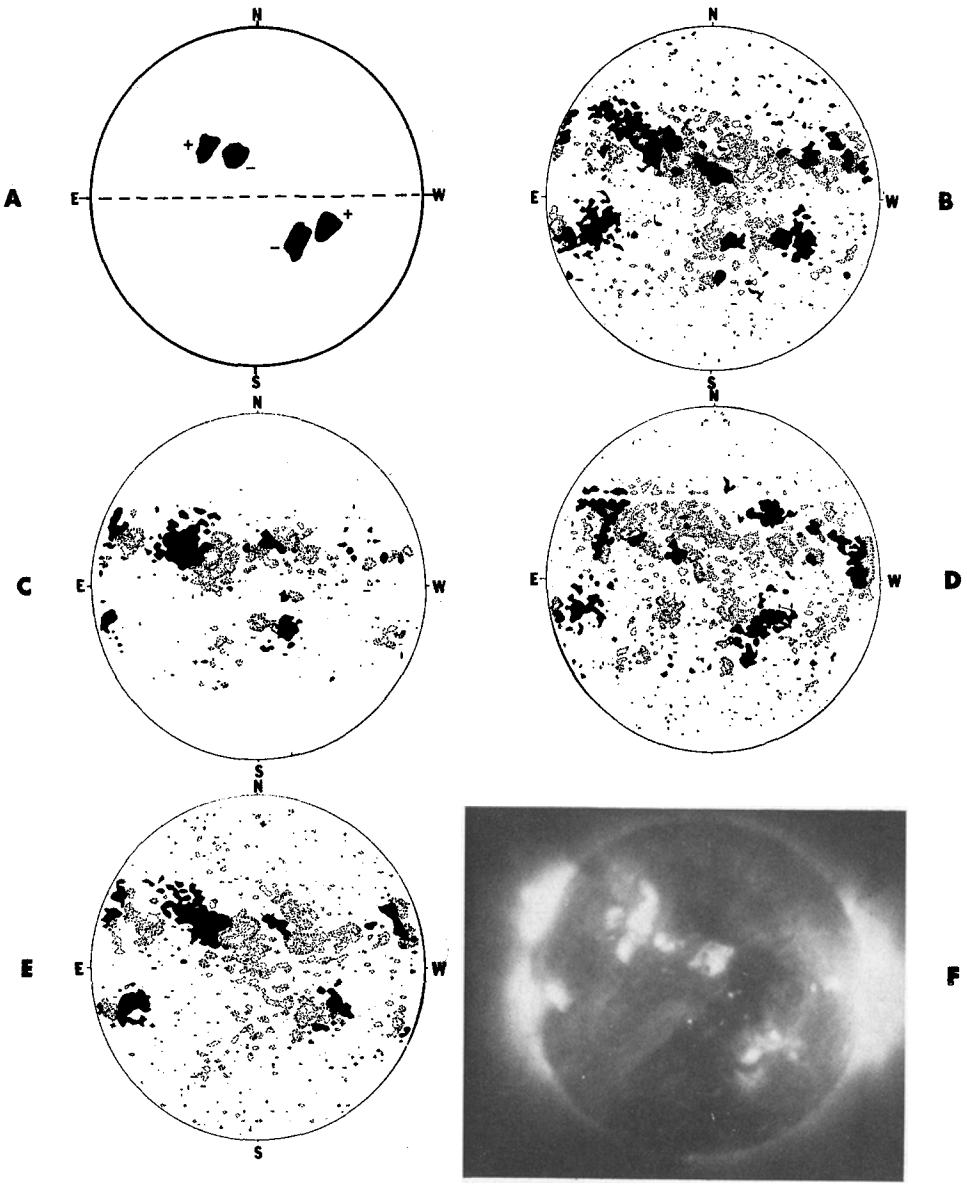

Fig. 6. (a) A schematic diagram of the active region magnetic field geometry resulting in the formation of the large scale patterns associated with the formation of the November 24, 1970 hole. (b, c, d, e) Mt. Wilson magnetograms for September 3, October 1, October 28, and November 23, 1970, respectively, showing the evolution of the actual field pattern during four successive solar rotations. (f) The soft X-ray observations of a coronal hole observed on November 24, 1970 from a solar sounding rocket. The X-ray bandpass is 3–35 and 44–51 Å. Magnetic field convention is: solid = plus polarity; dotted = minus polarity. (Mt. Wilson magnetograms are obtained from *Solar Geophysical Data*, 1970).

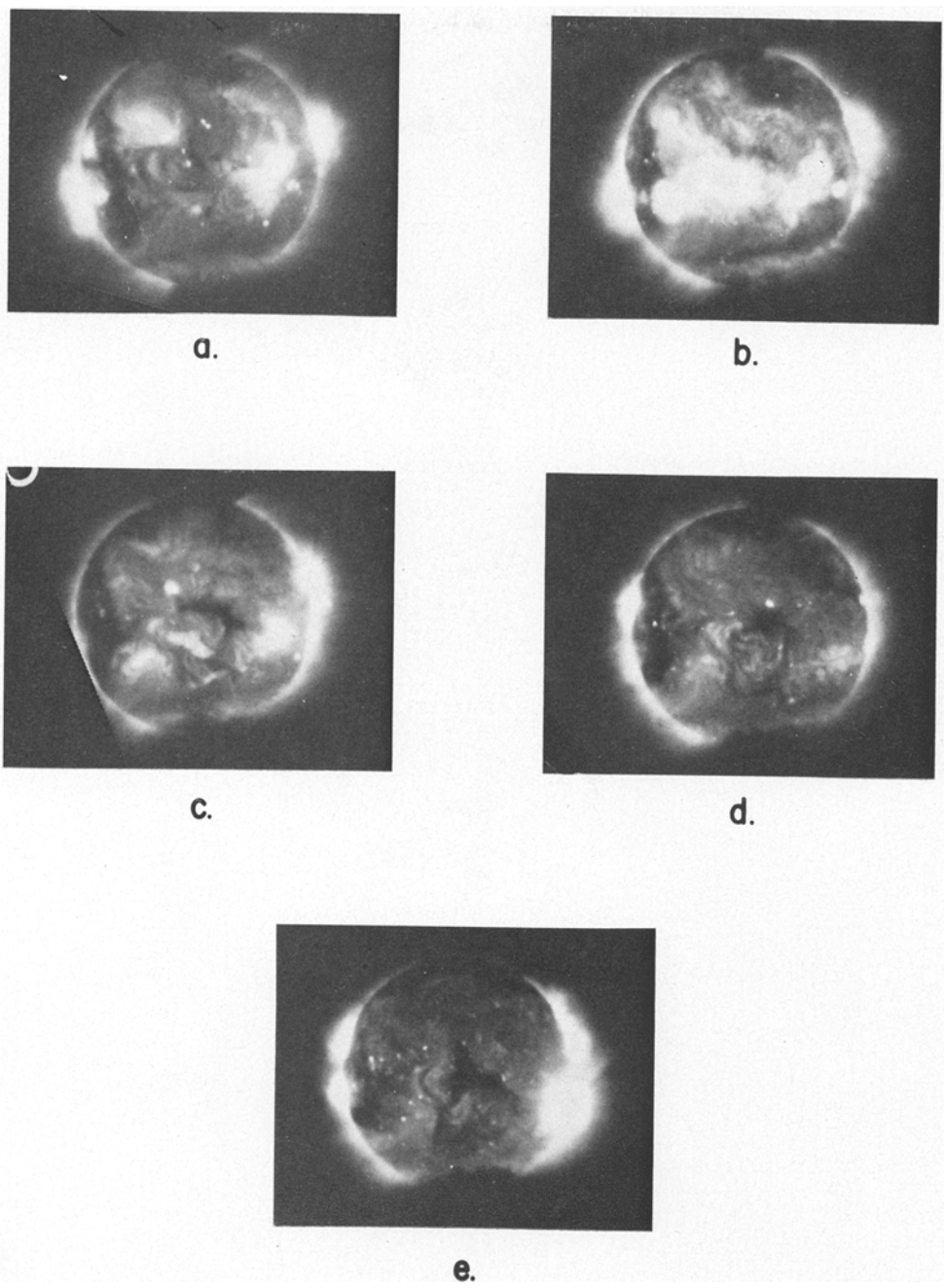

Fig. 7. Soft X-ray observations of the X-ray corona in the wavelength band 3–32 and 44–54 Å showing the formation and evolution of a completely enclosed coronal hole. The observations were obtained on May 28, 1973 at 0344 UT (a), June 23, 1973 at 1959 UT (b), July 21, 1973 at 0052 UT (c), August 17, 1973 at 0147 UT (d), and September 13, 1973 at 0200 UT (e).

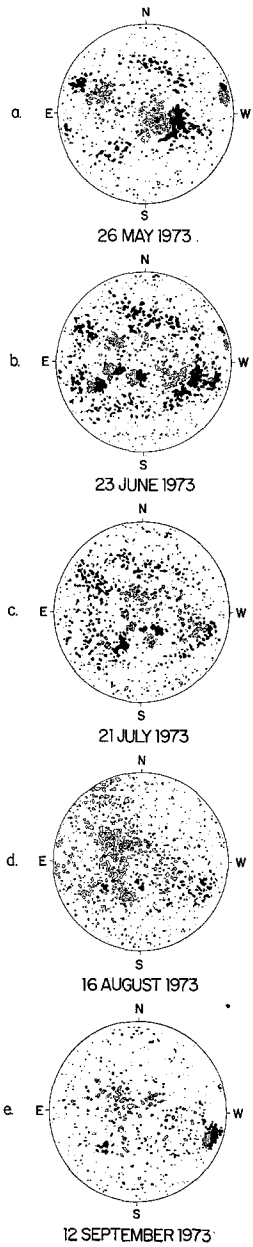

Fig. 8. Mt. Wilson magnetograms of the Sun obtained on May 26, 1973, June 23, 1973, July 21, 1973, August 16, 1973 and September 12, 1973 showing the formation and development of the large scale field pattern associated with the hole CH2 shown in Figure 7. Magnetic field convention is: solid = plus polarity; dotted = minus polarity. (Mt. Wilson magnetograms are obtained from *Solar Geophysical Data*, 1973).

fields which, in the south, form the northern boundary of the large polar filament cavity. It is possibly the presence of these fields which inhibits the poleward migration of the southern hemisphere negative field pattern of the hole and hence prevent the formation of an elongated hole similar to that of November 24, 1970.

2.3. Evolution

In order to determine the effect of the migration of active region remnant fields, of differential rotation and of the emergence of new, perturbing field patterns on the form and stability of a coronal hole, CH1 was observed throughout the first two Skylab missions. Images showing the feature near central meridian passage of five successive rotations are shown in Figure 9a. It is immediately apparent that the general form of the structures forming the hole boundaries changes significantly during the period shown. Active regions emerge in the southwest boundary during the second rotation and in the center of the hole during the third rotation producing field remnants which distort rather than reinforce the large scale field pattern. These observations suggest that CH1 finally narrows due to a reconnection of the magnetic structures comprising its western boundary with the active region remnants located within it. The time taken for these active region fields to diffuse to the hole boundaries is consistent with the 55 days predicted using a value of 10^4 km^2 s^{-1} for the rate of spread of the fields (Leighton, 1964).

On the eastern side of CH1 the emergence of active region flux also apparently affects the hole geometry. Comparison of the position of the hole boundaries after each 27 day rotation period shows that as the initial active regions decay on the eastern edge of the hole, the boundary moves eastward. However, when the new active regions emerge somewhat to the east of the boundary during the fourth and fifth rotations they appear to inhibit further expansion of the hole in this direction. At latitudes above the active region zone (latitudes ϕ greater than 30–35°N) some evidence of differential rotation is seen.

The northwestern extremity of the hole boundary ($\phi \sim 50$–$60°$N) is seen to be particularly variable in latitude from one rotation to the next. It is, however, difficult to determine from Figure 9 whether the changes seen are a result of the restructuring of magnetic fields or of an intensity variation in pre-existing loop structure. The situation can, to some extent, be clarified by studying the boundary in question with higher time resolution. Four views of the hole during its August disk passage are shown in Figure 10. Definite evidence is seen of a loop structure becoming detached from the northwestern boundary and apparently moving into the hole. Thus, at these latitudes, magnetic restructuring can be seen to occur at the hole boundary.

2.4. Rotation

It is apparent from Figure 9a that while the structures which delineate the hole boundary change significantly with time, the position of the hole boundary itself retains its identity and appears to rotate as a rigid body with only slight distortion due to differential rotation. The difference between the actual rotation characteristics

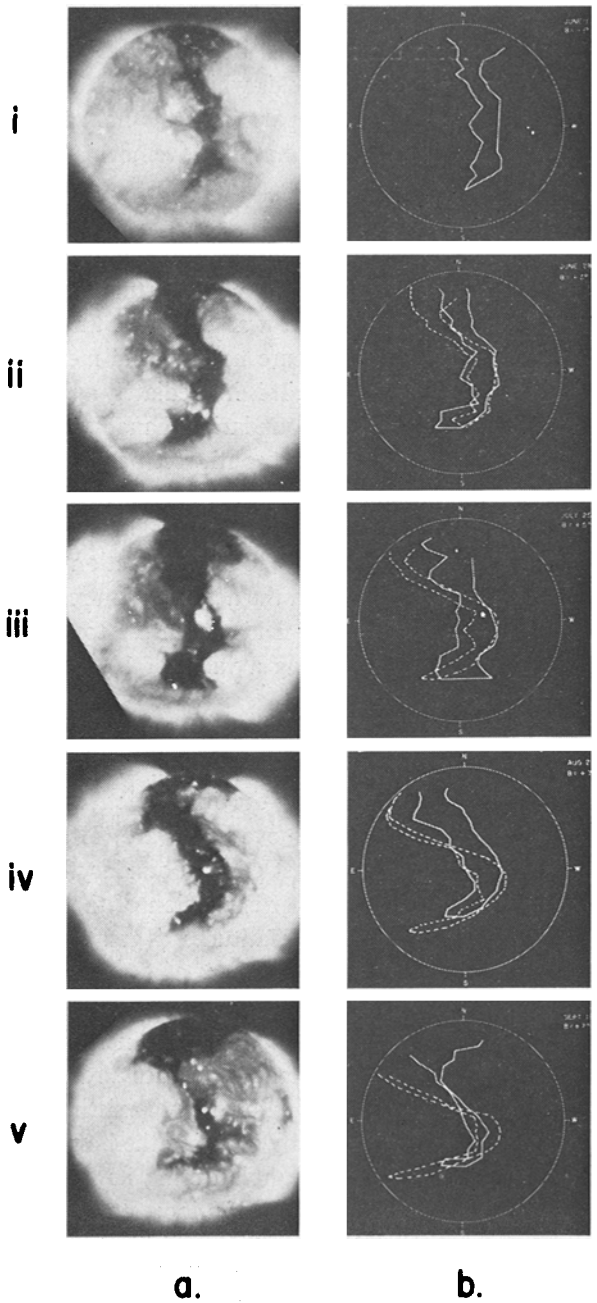

Fig. 9. Comparison of the position of CH1 as seen (a) in soft X-ray wavelengths 3–32 Å and 44–54 Å and (b) its extrapolated position calculated using the Newton and Nunn (1951) differential sunspot rotation rates. Images are shown in five successive rotations for: (i) June 1, 1973; (ii) June 28, 1973; (iii) July 25, 1973; (iv) August 21, 1973; and (v) September 28, 1973. The solid line on each schematic represents the outline of the hole as measured on that rotation, the dotted line shows the extrapolated position of the hole measured on the first rotation and rotated through the appropriate time interval.

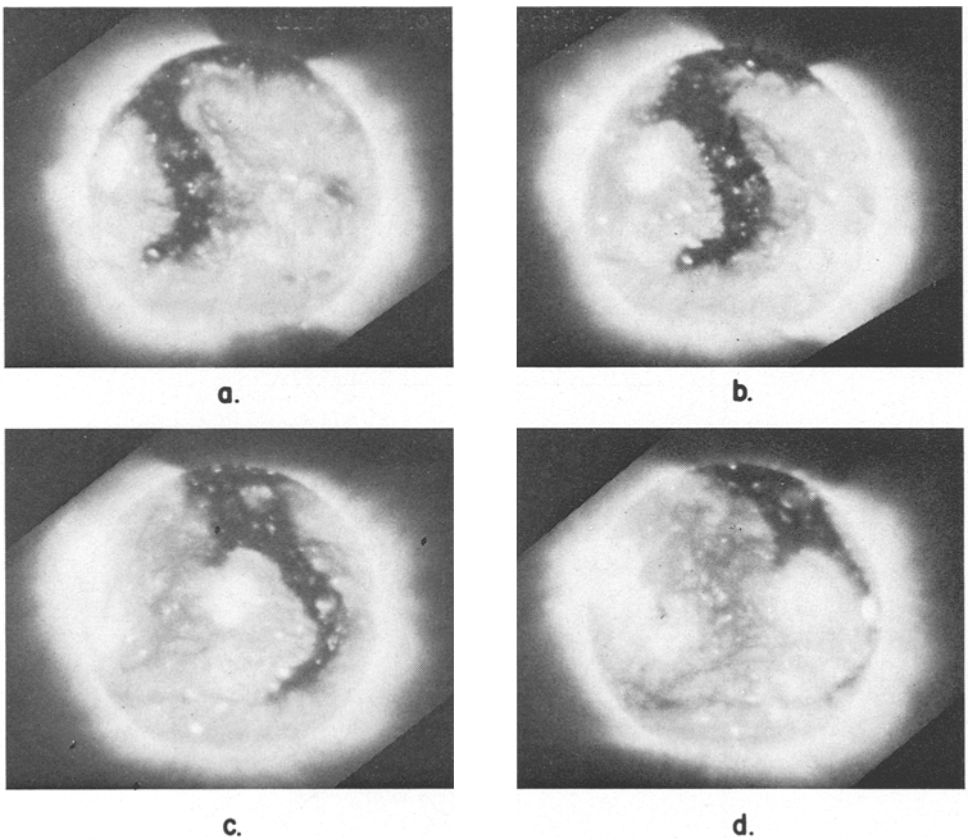

Fig. 10. Soft X-ray images (3–32 and 44–54 Å) showing short term changes in structure in the northwest boundary of CH1. Observations marked (a), (b), (c) and (d) correspond to August 19, 1973, 1309 UT; August 21, 1973, 0041 UT; August 23, 1973, 1328 UT; and August 25, 1973, 1226 UT, respectively.

of the hole and the normal differential rotation can best be illustrated by computing the form of CH1 as it would appear on its four successive rotations, if it were rotating with the sunspot differential rotation rate, and comparing this with our actual observations of the feature. The results of this comparison are shown in Figure 9b.

It is possible to determine the rotation rate of the coronal hole as a function of latitude by noting the period between successive central meridian transits of the boundaries of the hole at any latitude. In order to do this, we have generated a series of plots, which show the longitude of the eastern and western boundary of the hole as a function of time for each 5° interval of latitude from 60° N to 25° S. One such plot (for the equator, on the fourth disk passage of the hole) is shown in Figure 11. The time of central meridian passage (CMP) of the hole boundary is determined by the best fit to these data. As will be discussed below, we also determine the X-ray emission scale height (one-half the density scale height) of the closed coronal structures bound-

ing the hole by this procedure. The scatter of the points shown in Figure 11 is primarily due to the difficulty of judging the position of the edge of optically thin structures. Temporal variations in boundary structures also contribute to this scatter.

From the CMP timings, we then determine a best fit constant rotation rate for each latitude, treating the eastern and western boundaries of the coronal hole separately. The resulting synodic rotation rates are shown in Figure 12. The large error

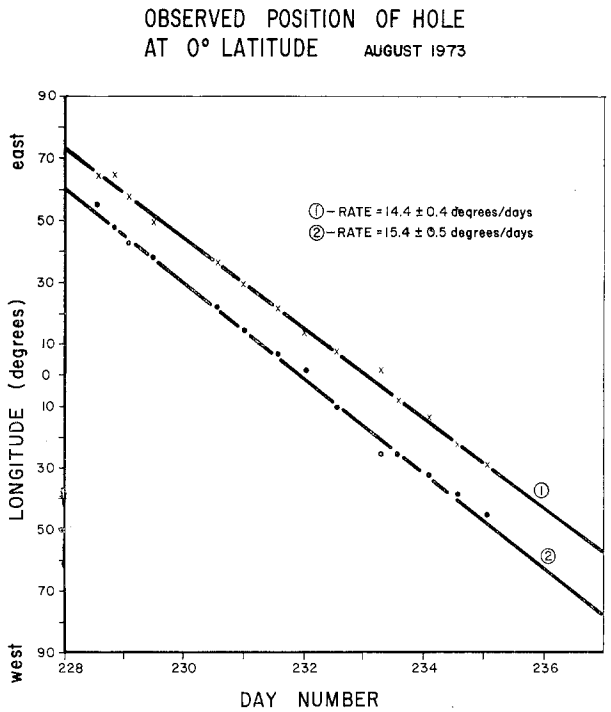

Fig. 11. Measured disk transit rates for the east and west equatorial boundaries of the coronal hole during its August 1973 disk crossing.

bars for 55° N and 60° N are due to the temporal changes at these latitudes, mentioned previously. For comparison, we have included the generally accepted sunspot rotation rates of Newton and Nunn (1951). Even if we ignore the points at 55° and 60°, it is apparent that the observed rotation rates for the coronal hole display substantially less differential rotation than the Newton and Nunn rates. The best fit to the coronal hole data over five rotations (from 20° S to 50° N) gives a synodic rotation rate of $13.25 \pm 0.03 - (0.4 \pm 0.1) \sin^2 \phi$ deg day^{-1}, where ϕ is the latitude. This is to be compared with the sunspot rate of $13.39 - 2.7 \sin^2 \phi$ deg day^{-1}. The coronal hole boundaries rotate in an almost rigid manner compared to the sunspots.

The apparent rotation rates deduced from the plots of longitude as a function of

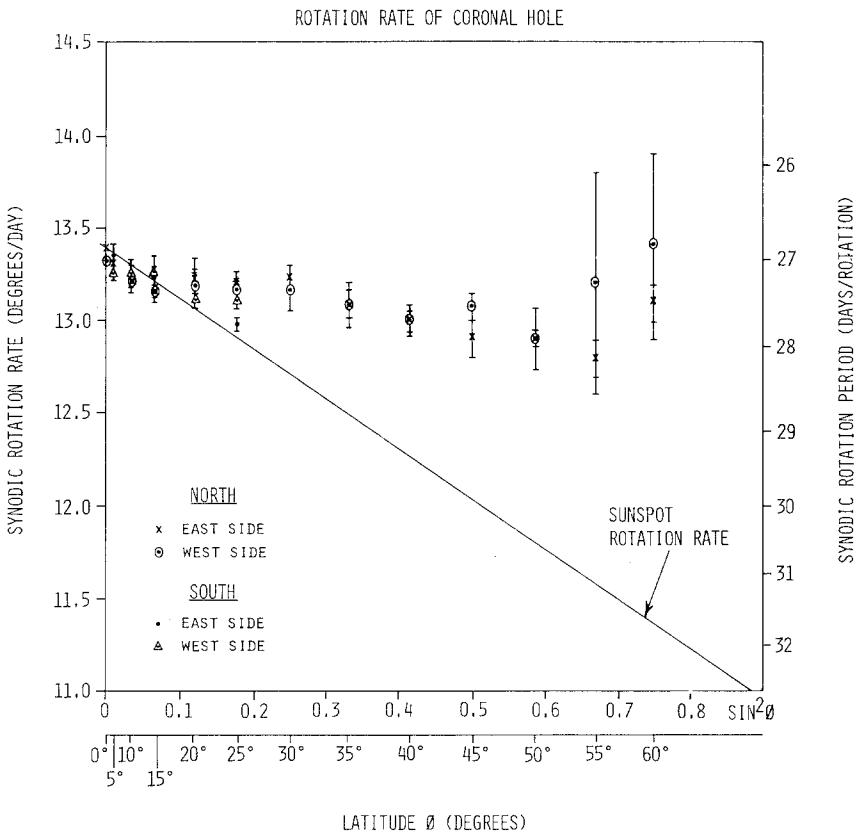

Fig. 12. True rotation rate of CH1 as a function of latitude determined from measurements of the times of central meridian passage of the boundary structures for the period May 28 to September 20, 1973.

time (such as Figure 11) are functions not only of the true rotation rate, but also of the finite thickness of the boundary structures. An approximate geometry for the simple case of a vertical structure at the equator is shown in Figure 13. Once the true rotation rate $(d\beta/dt)$ is known, the average emission scale height $(x-R_\odot)$ at latitude ϕ can be determined from the apparent rotation rate $(d\alpha/dt)$, by means of the relationship:

$$\frac{x}{R_\odot} = \left\{1 + (1 - \cos^2\alpha\cos^2\phi)\left[\frac{(d\beta/dt)^2}{(d\alpha/dt)^2} - 1\right]\right\}^{1/2} \Big/ \left\{\frac{(d\beta/dt)}{(d\alpha/dt)}\right\}$$

which can be derived from examination of Figure 13. We find that the emission scale heights of the closed structures forming the coronal hole boundaries lie typically in the range from 5×10^4 km to 8×10^4 km. This is in good agreement with the values which we have reported previously (Krieger *et al.*, 1973) for the X-ray emission scale heights of closed coronal structures measured directly at the solar limb.

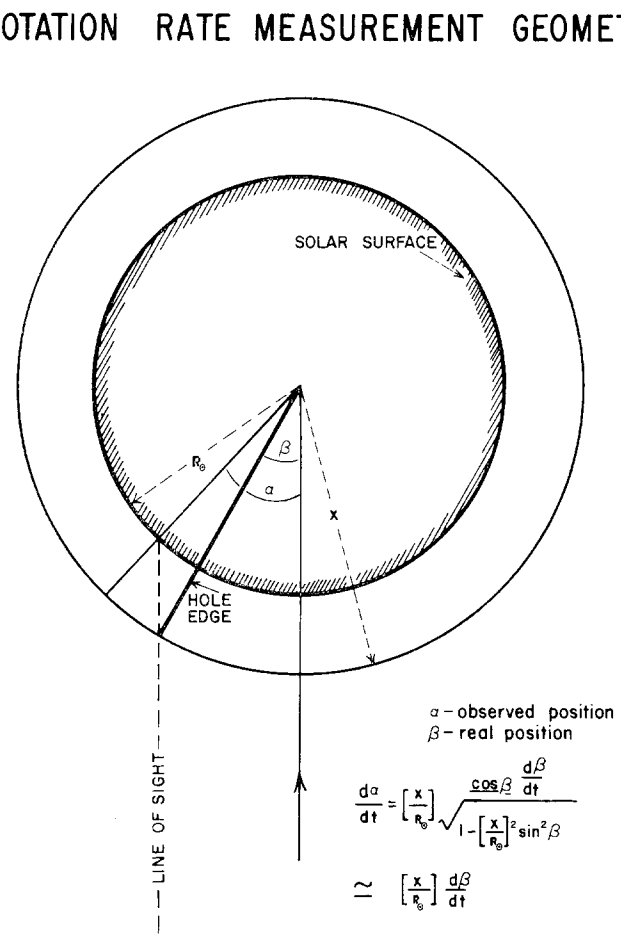

Fig. 13. Geometrical representation of the hole and boundary structures for the equatorial case assuming a spherically symmetrical boundary of uniform thickness $x-R_\odot$.

3. Summary of Results

Analysis of our ATM soft X-ray observations shows that coronal holes are open features with a divergent magnetic field configuration which results from a particular large scale magnetic field topology. They seem to be formed when the successive emergence and dispersion of active region fields produces a swath of unipolar field, bounded by fields of opposite polarity, and die when large scale field patterns emerge which significantly distort the original field configuration. The lifetime of the holes, like that of the large scale magnetic features with which they are associated, is typically of the order of many solar rotations.

Two configurations of holes are seen. The first type are compact features which are almost completely enclosed by fields of opposite polarity and lie predominantly in one hemisphere of the Sun. In addition, elongated holes occur which have a north-

south orientation and extend approximately 110–120° in latitude from one pole to mid latitudes in the opposite hemisphere where they are terminated by an east-west oriented filament channel.

A five month study of one particular elongated hole (CH1) showed that the hole as an entity exhibited only slight evidence of differential rotation. This is puzzling because the character of the structures comprising its boundary changed significantly with time, exhibiting emergence of new magnetic flux, local variations in rotation rate, and magnetic field reconfigurations.

4. Coronal Rotation

Evidence for deviations in the corona from the photospheric pattern of differential rotation with latitude has been obtained before. These results were obtained by autocorrelation of limb intensities of the white light (Hansen *et al.*, 1969) and green line (Antonucci and Svalgaard, 1974) coronas. Such results are heavily dependent on statistics in that changes in coronal structure, particularly those occurring in the longitudinal direction, introduce uncertainties into the analysis of individual features. To our knowledge, the result presented here is the first direct observation of deviation from the differential rotation law for a specific coronal feature. There appear to be several different possible mechanisms for this phenomenon which are consistent with our data.

Evidence for the 'rigid rotation' of certain long lived solar features has also been found by Wilcox and his co-workers in their studies of solar magnetic sector structures (Wilcox and Tannenbaum, 1971; Svalgaard, 1972). In addition, Wilcox *et al.* (1970) have interpreted an autocorrelation analysis of large scale photospheric magnetic fields in terms of both a differentially rotating component and a rigidly rotating component. In their study the former are associated with active region fields and their remnants and correspond to the original Wilcox and Howard (1970) analysis. The rigid rotation is associated with longer lived weak field features.

Bumba and Howard (1969) have postulated the existence of rigidly rotating 'subsurface sources' covering tens of degrees in latitude and longitude in order to account for long lived features in the photospheric field pattern and as an explanation for 'active longitudes' (Dodson-Prince and Hedeman, 1968; Švestka, 1968). Such structures have been invoked to explain the rotation properties of the weak photospheric fields and their existence may be consistent with some formulations of the solar dynamo theory (Wilcox, private communication).

One can then ask whether our observations of the almost rigid rotation of a long-lived coronal hole are consistent with the hypothesis of a rigidly rotating subsurface feature. In our view the evidence is not conclusive. We note that although the photospheric magnetic field in the coronal hole region itself is generally weak, the hole is bounded in many areas by active regions and recent active region remnants. Because these features have relatively strong fields, they should exhibit differential rotation, based on the arguments of Wilcox *et al.* (1970) and of Bumba and Howard (1969).

However, our observations show that the location of the hole boundaries differ significantly from the positions predicted by the normal differential rotation law (Figure 9). There is some indication, however, from observations such as those of Figure 10, that the coronal structures associated with closed magnetic field formations which we use to observationally delimit the boundaries of the hole actually 'move through' the hole (see Section 2.3). This implies that the hole (defined as the open field region and not the boundary structures) might indeed be the manifestation of a more deep seated structure rotating at a different rate from the surface. Furthermore, holes are seen to be associated with large scale weak field patterns which are reinforced by successive emergence and dispersal of active region fields. Thus, if the form and rotational characteristics of such large scale weak field features can be attributed to a deep seated structure (Bumba and Howard, 1969) then holes may also be a manifestation of this structure. A critical observation which may help this paradox will be the identification of the supergranulation network elements comprising the footpoints of the coronal boundary loop structures and an investigation of their evolution and of their rotational characteristics.

Newkirk (1967) has suggested that closed coronal magnetic field lines which interconnect regions of different latitude will tend to bring these regions more nearly to the same angular velocity than is the case for the underlying photosphere. Pneuman (1971) has computed the angular velocity distribution along such a field line for some simple geometries. His results imply that the rotation rate will increase monotonically along a field line from its high latitude footpoint to its low latitude footpoint and that this will tend to wash out the differential rotation of the solar atmosphere. This mechanism might explain the deviation of the coronal hole rotation pattern from the photospheric differential law. We regard this as unlikely, however, because there is evidence that the field lines of the coronal hole are open to the interplanetary medium both from examination of the magnetic field extrapolations of Newkirk *et al.* (1973) and the relationship between the coronal holes and high speed solar wind streams (Krieger *et al.*, 1973; Neupert and Pizzo, 1974; Krieger *et al.*, 1974).

Weber and Davis (1967) and Weber (1969) have considered the relationship between the angular velocity of the plasma moving along a coronal magnetic field line and its angular momentum and magnetic torques. In general, the angular velocity of the corona is shown to decrease with height on an open field line. Weber (1969) has calculated, however, that in the case of a strongly divergent field configuration, the angular velocity may increase with height near the solar surface. We find the presence of a strongly divergent field configuration to be a general property of coronal holes. The white light and X-ray coronal photographs superimposed by Van Speybroeck *et al.* (1970) show a graphic example of this phenomenon. Thus, one may speculate that the deviation of the rotation properties of the coronal hole from the photospheric differential pattern may be a manifestation of a mechanism similar to that suggested by Weber (1969).

The almost complete absence of latitude dependence in the rotation rate of CH1 might therefore be a manifestation of any of three different classes of mechanisms:

(1) a rigidly rotating subphotospheric phenomenon exemplified by the type suggested by Bumba and Howard (1969); (2) a linking of high and low latitudes by closed field lines as typified by the suggestion of Pneuman (1971): or (3) an interaction between moving coronal material and open field lines such as the suggestion of Weber (1969). While the present analysis cannot distinguish between these classes of mechanisms, the high resolution X-ray images of ATM permit detailed numerical evaluation of the consequences of such mechanisms in terms of actual coronal structures and their measured rotation rates.

Acknowledgements

We would like to thank Dr J. Harvey and Dr W. Livingston of Kitt Peak National Observatory for the provision of their magnetic field data. We are also grateful to Dr J. Wilcox of the Institute for Plasma Research, Stanford University and Dr G. Noci of Arcetri Astrophysical Observatory for helpful discussions. At AS & E we are indebted to Mr R. Haggerty and his team of photographers for their support in the photographic processing and display of the X-ray data and to Mrs P. Wetherbee for her assistance in the preparation of data for this document. This work has been supported by NASA, Marshall Space Flight Center under contract NAS8-27758.

References

Altschuler, M. D., Trotter, D. E. and Orrall, F. Q.: 1972, *Solar Phys.* **26**, 354.
Antonucci, E. and Svalgaard, L.: 1974, *Solar Phys.* **34**, 3.
Babcock, H. W.: 1961, *Astrophys. J.* **133**, 572.
Bumba, V. and Howard, R.: 1969, *Solar Phys.* **7**, 28.
Dodson-Prince, H. W. and Hedeman, E. R.: 1968, in K. O. Kiepenheuer (ed.), 'Structure and Development of Solar Active Regions', *IAU Symp.* **35**, 56.
Dulk, G. A. and Sheridan, K. V.: 1974, *Solar Phys.* **36**, 191.
Golub, L., Krieger, A. S., Silk, J. K., Timothy, A. F., and Vaiana, G. S.: 1974, *Astrophys. J.* **189**, L93.
Hansen, R. T., Hansen, S. F., and Loomis, H. G.: 1969, *Solar Phys.* **10**, 135.
Harvey, J., Krieger, A. S., Timothy, A. F., and Vaiana, G. S.: 1974, 'Comparison of Skylab X-ray and Ground Based Helium Observations', to be published in the *Proceedings of the Working Session on the Preliminary Results of the Skylab Solar Experiments and Correlated Ground Observations*, Arcetri Astrophysical Observatory, Florence, Italy.
Krieger, A. S., Timothy, A. F., and Roelof, E. C.: 1973, *Solar Phys.* **29**, 505.
Krieger, A. S., Timothy, A. F., Vaiana, G. S., Lazarus, A. J., and Sullivan, J. D.: 1974, in *Proceedings of the Third Solar Wind Conference at Asilomar Conference Grounds*, California.
Leighton, R. B.: 1964, *Astrophys. J.* **140**, 1547.
Munro, R. H. and Withbroe, G. L.: 1972, *Astrophys. J.* **176**, 511.
Neupert, W. M. and Pizzo, V.: 1974, to be published in *J. Geophys. Res.*
Newkirk, G. A.: 1967, *Ann. Rev. Astron. Astrophys.* **5**, 213.
Newkirk, G., Jr., Trotter, D. E., Altschuler, M. D., and Howard, R.: 1973, 'A Microfilm Atlas of Magnetic Fields in the Solar Corona', NCAR Technical Note, NCAR-TN/STR-85.
Newton, H. W. and Nunn, M. L.: 1951, *Monthly Notices Roy. Astron. Soc.* **111**, 413.
Pneuman, G. W.: 1971, *Solar Phys.* **19**, 16.
Svalgaard, L.: 1972, *J. Geophys. Res.* **77**, 4027.
Švestka, Z.: 1968, *Solar Phys.* **4**, 18.
U.S. Department of Commerce, Environmental Science Services Administration: 1973, *Solar Geophyscial Data*, pp. 345–7.
Vaiana, G. S , Krieger, A. S., and Timothy, A. F.: 1973a, *Solar Phys.* **32**, 81.

Vaiana, G. S., Davis, J. M., Giacconi, R., Krieger, A. S., Silk, J. K., Timothy, A. F., and Zombeck, M.: 1973b, *Astrophys. J.* **185**, L47.
Van Speybroeck, L. P., Krieger, A. S., and Vaiana, G. S.: 1970, *Nature* **227**, 818.
Weber, E. J.: 1969, *Solar Phys.* **9**, 150.
Weber, E. J. and Davis, L., Jr.: 1967, *Astrophys. J.* **148**, 217.
Wilcox, J. M. and Howard, R.: 1970, *Solar Phys.* **13**, 251.
Wilcox, J. M. and Tannenbaum, A. S.: 1971, *Space Sci. Lab. Rep. Ser.* **12**.
Wilcox, J. M., Schatten, K. H., Tannenbaum, A. S., and Howard, R.: 1970, *Solar Phys.* **14**, 255.